



Published in final edited form as:

*J Immunol.* 2024 November 01; 213(9): 1358–1370. doi:10.4049/jimmunol.2400417.

## Intravenous BCG induces a more potent airway and lung immune response than intradermal BCG in SIV-infected macaques

Solomon Jauro<sup>\*,†,2</sup>, Erica C. Larson<sup>\*,†</sup>, Janelle L. Gleim<sup>\*</sup>, Brendon M. Wahlberg<sup>\*</sup>, Mark A. Rodgers<sup>\*</sup>, Julia C. Chehab<sup>\*</sup>, Alondra E. Lopez-Velazquez<sup>‡</sup>, Cassaundra L. Ameel<sup>\*</sup>, Jaime A. Tomko<sup>\*</sup>, Jennifer L. Sakal<sup>\*</sup>, Todd DeMarco<sup>§</sup>, H. Jacob Borish<sup>\*</sup>, Pauline Maiello<sup>\*</sup>, E. Lake Potter<sup>¶</sup>, Mario Roederer<sup>¶</sup>, Philana Ling Lin<sup>†,||</sup>, JoAnne L. Flynn<sup>\*,†</sup>, Charles A. Scanga<sup>\*,†,2</sup>

<sup>\*</sup>Department of Microbiology and Molecular Genetics, University of Pittsburgh, School of Medicine, Pittsburgh, PA, USA.

<sup>†</sup>Center for Vaccine Research, University of Pittsburgh, School of Medicine, Pittsburgh, PA, USA.

<sup>‡</sup>Department of Biology, University of Puerto Rico – Humacao Campus, Puerto Rico, USA.

<sup>§</sup>Human Vaccine Institute, Duke University School of Medicine, Durham, NC, USA.

<sup>¶</sup>Vaccine Research Center, National Institute of Allergy and Infectious Diseases (NIAID), National Institutes of Health (NIH), Bethesda, MD, USA.

<sup>||</sup>Department of Pediatrics, Children's Hospital of Pittsburgh of the University of Pittsburgh Medical Center, University of Pittsburgh, School of Medicine, Pittsburgh, PA, USA.

### Abstract

Tuberculosis (TB), caused by *Mycobacterium tuberculosis* (Mtb), is one of the leading causes of death due to an infectious agent. Coinfection with HIV exacerbates Mtb infection outcomes in people living with HIV (PLWH). Bacillus Calmette-Guérin (BCG), the only approved TB vaccine, is effective in infants, but its efficacy in adolescents and adults is limited. Here, we investigated the immune responses elicited by BCG administered via intravenous (IV) or intradermal (ID) routes in Simian Immunodeficiency Virus (SIV)-infected Mauritian cynomolgus macaques (MCM) without the confounding effects of Mtb challenge. We assessed the impact of vaccination on T cell responses in the airway, blood, and tissues (lung, thoracic lymph nodes, and spleen), as well as the expression of cytokines, cytotoxic effectors, and key transcription factors. Our results showed that IV BCG induces a robust and sustained immune response, including tissue-resident memory T (T<sub>RM</sub>) cells in lungs, polyfunctional CD4<sup>+</sup> and CD8αβ<sup>+</sup> T cells expressing multiple cytokines, and CD8αβ<sup>+</sup> T cells and NK cells expressing cytotoxic effectors in airways. We also detected higher levels of mycobacteria-specific IgG and IgM in the airways of IV BCG-vaccinated MCM. Although IV BCG vaccination resulted in an influx of T<sub>RM</sub> cells in lungs of MCM with controlled SIV replication, MCM with high plasma SIV RNA (>10<sup>5</sup> copies/mL) typically displayed reduced T cell responses, suggesting that uncontrolled SIV or HIV replication would have a detrimental effect on IV BCG-induced protection against Mtb.

<sup>2</sup>Corresponding Authors: s\_jauro@pitt.edu, scangaca@pitt.edu.

## Keywords

BCG; vaccination; SIV/HIV; macaques; tissue-resident memory T cell

## Introduction:

Tuberculosis (TB) remains a major infectious cause of mortality globally. Over one-fourth of the world's population is estimated to be or have been infected with *Mycobacterium tuberculosis* (Mtb), the causative agent of TB, and over 10 million new cases of active TB are reported yearly. In 2022, TB resulted in the death of 1.6 million people (1). TB disease is exacerbated in people living with HIV (PLWH), with morbidity rates 15 – 21 times higher than HIV-naïve individuals (2). PLWH have a higher likelihood of progression from latent to active TB as well as higher mortality rates, contributing to one out of three deaths in PLWH (1, 3). This grave effect of TB in PLWH correlates with the extent to which HIV infection depletes CD4+ T cells, an important cell type in host immunity against Mtb. CD4+ T cells are considered important for TB protection as HIV-mediated depletion of these cells results in rapid TB progression in PLWH (4, 5). However, even in some PLWH with normal CD4+ T cell levels (500–1500 cells/mm<sup>3</sup>), TB progression is more rapid than in HIV-naïve individuals (6). This may result from HIV-related factors that affect immunity, including impairment of anti-mycobacterial innate immunity by type I interferon (7, 8), immune suppression due to Treg/Th17 imbalances (9), interference of B cell signaling and memory formation (10), and inhibition of TNF-mediated macrophage activation and death (11, 12). A safe and effective TB vaccine would greatly reduce the risk of TB and mortality in PLWH and would significantly improve global health. Yet, HIV impairment of vaccine-elicited responses is not completely understood.

Bacillus Calmette-Guérin (BCG) is the only licensed vaccine for TB and was developed over a century ago. BCG is delivered intradermally (ID) to infants worldwide and is effective against severe TB in children, but its efficacy diminishes into adulthood (1). Many studies are focused on improving BCG efficacy. Clinical studies of BCG revaccination and protein subunit vaccines that examined sustained Quantiferon-TB conversion or prevention of latent TB progression to active TB demonstrated moderate vaccine efficacy of 30–50% in HIV-naïve subjects (13, 14). In nonhuman primates (NHP), BCG boosted with Mtb proteins improved T cell responses in the lungs but did not enhance protection from Mtb challenge (15). However, a study of BCG vaccination delivered by different routes in rhesus macaques revealed the intravenous (IV) route to be the most protective, conferring 90% protection from TB (16). Despite these encouraging results, BCG, being a live attenuated vaccine, has the potential to cause disease in immunocompromised individuals. The risk of disseminated BCG in infants infected with HIV is significantly higher than in infants who are HIV-naïve (17), prompting safety concerns for BCG as a vaccine for immunocompromised persons (18). Nonetheless, we recently showed that IV BCG in MCM chronically infected with simian immunodeficiency virus (SIV), an NHP surrogate for HIV, was safe (at least with anti-BCG drug treatment post-vaccination), immunogenic, and protective (19).

Understanding vaccine-elicited immune responses that correlate with TB protection is critical for rational vaccine development. Several features have been associated with TB protection in IV BCG-vaccinated, SIV-naïve rhesus macaques, including an influx of mycobacterial-specific T cells into the airways and expansion of  $T_{RM}$  cells in lung tissue (16, 20), elevation of mycobacterial-specific antibodies in circulation and in airway (21), and distinct transcriptional profiles in circulating PBMC (22). In a correlates analysis across a dose range of IV BCG, CD4 T cells expressing different combinations of  $IFN\gamma$ , TNF and/or IL-17 as well as the number of NK cells in airways were correlates of protection independent of BCG dose (20). In our study of IV BCG in SIV-infected MCM (16), TB protection tended to occur in animals with lower plasma viremia and higher levels of CD4+ T cells in the airways before Mtb challenge. Although we were able to assess vaccine responses in blood and airway, all animals underwent Mtb challenge, thereby complicating assessment of immune responses within tissues.

Here, we evaluated immune responses to BCG in MCM chronically infected with SIV following vaccination delivered either IV or the standard ID route, and BCG responses in tissues were analyzed without subsequent Mtb challenge. We used our well-characterized MCM model of SIV/Mtb coinfection (23–28) and infected the animals with SIV for 16 weeks before IV or ID BCG vaccination. Blood and airway cells were serially sampled, and animals were necropsied 5 months after vaccination to compare the immune response within various tissues between ID and IV BCG in SIV-infected MCM. We show that vaccination of SIV-infected MCM with IV BCG elicited an influx of CD4+, CD4+CD8 $\alpha$ +, CD8 $\alpha$ α+, CD8 $\alpha$ β+, and V $\gamma$ 9+ $\gamma$ δ, V $\gamma$ 9- $\gamma$ δ T cells, and cytokine-producing CD4+ and CD8 $\alpha$ β+ T cells into the airways. Airway immune responses by IV BCG were mostly recapitulated in lung tissues with an expansion of CD8 $\alpha$ α+, CD8 $\alpha$ β+, and  $\gamma$ δ+  $T_{RM}$  cells.

## Materials and Methods

### Animals:

Eleven (11) male MCM (*Macaca fascicularis*, 4–10 years old) were procured from Bioculture US (Immokalee, FL). Major histocompatibility complex (MHC) haplotypes, which were determined by MiSeq sequencing of PBMC at the Genomic Services Core of the Wisconsin National Primate Research Center, and 8 the 11 MCM shared at least one copy of the M1 MHC haplotype. The MCM were screened for Mtb, as well as herpes B virus, SIV, SRV, and STLV, and housed at the University of Pittsburgh. All experimental procedures were conducted according to the ethical regulations of the University of Pittsburgh Institutional Animal Care and Use Committee (IACUC), and complied with the standards outlined in the Animal Welfare Act, the “Guide for the Care and Use of Laboratory Animals (8<sup>th</sup> Edition)”, and “The Weatherall Report”. The University is fully accredited by AAALAC (accreditation number 000496), and its OLAW animal welfare assurance number is D16–00118. The IACUC reviewed and approved the study protocols 21048970 and 24044961. All veterinary procedures were performed under ketamine sedation. The MCM were monitored twice daily for any health issues.

**SIV infection:**

All MCM were infected intravenously with a  $3 \times 10^3$  tissue culture infectious dose (TCID<sub>50</sub>) of SIVmac239 which was grown in rhesus PBMC (Primate Assay Laboratory of the California National Primate Research Center, University of California, Davis CA). Plasma virus level was serially monitored by qPCR, as detailed below.

**BCG vaccination:**

Sixteen weeks after SIV infection, the MCM were randomly allocated into two vaccination groups: IV BCG (n=5), and ID BCG (n=6) (Figure 1a). Animals were vaccinated with BCG Danish Strain 1331, which was expanded at Colorado State University following the Aeras protocol (29). The BCG was prepared for injection by suspending in phosphate-buffered saline (PBS) containing 0.05% Tween 80 (Sigma-Aldrich) to prevent the inoculum from clumping. For ID inoculations, the upper arm was shaved and disinfected with chlorhexidine followed by isopropanol, and the standard human dose of  $5 \times 10^5$  CFU was injected into the dermis in a volume of 1 mL. For IV inoculation, the saphenous vein was used to inject  $5 \times 10^7$  CFU in 1 mL total volume, the dose we showed previously to confer high-order protection in SIV-infected MCM (17). To reduce the risk of BCG dissemination in these SIV-infected animals, the IV BCG-vaccinated MCM were treated with an anti-BCG drug regimen (isoniazid, 15mg/kg; rifampicin, 20mg/kg; ethambutol, 55mg/kg (HRE)) given by mouth daily for 8 weeks starting 3 weeks after vaccination, as done previously (17).

**Sampling blood and airways:**

Whole blood was collected by venipuncture. PBMC were isolated using Ficoll-Paque PLUS gradient separation (GE Healthcare Biosciences) and cryopreserved in RPMI 1640/fetal bovine serum (FBS) containing 10% DMSO in liquid nitrogen. Bronchoalveolar lavage (BAL) was done by instilling and recovering warmed PBS ( $4 \times 10$  mL washes) under direct visualization using a pediatric bronchoscope. The recovered BAL fluid (BALF) was pelleted to collect the cells and a 15 mL aliquot of BALF was cryopreserved. The cells were resuspended into ELISpot media (RPMI 1640, 10% heat-inactivated human albumin, 1% L-glutamine, and 1% HEPES), counted, and apportioned for flow cytometric staining.

**PET-CT:**

PET-CT imaging using radiolabeled 2-deoxy-2-<sup>18</sup>Fluoro-D-glucose (FDG) was conducted within 3 days of necropsy. A MultiScan LFER-150 PET-CT scanner (Mediso Medical Imaging Systems, Budapest, Hungary) was used, as detailed previously (30, 31). Co-registered PET-CT images were analyzed using OsiriX MD software (v 12.5.2, Pixmeo, Geneva, Switzerland) to measure the total FDG avidity of the lungs, thoracic lymph nodes (32). Total FDG avidity correlates with overall inflammation.

**IV CD45 staining for tissue-resident cells:**

To differentiate T<sub>RM</sub> cells from intravascular cells, IV anti-CD45 antibody staining was performed as previously described (16, 33, 34). Briefly, 5 minutes before euthanasia, animals were maximally bled and then slowly infused intravenously with 5 mL of purified Alexa Fluor 488-conjugated αCD45 antibody to achieve a dose of 100 μg/kg. For the

ID BCG vaccination group, 5 of 6 MCM were injected IV with anti-CD45 antibodies. When harvested tissues were analyzed by flow cytometry, CD45 immune cells present in parenchyma were unstained, while those in the vascular were positively stained with anti-CD45 antibody.

### **Necropsy and tissue processing:**

Five months after vaccination, animals were humanely euthanized and necropsied to collect lung tissue, thoracic and peripheral lymph nodes, liver, and spleen. Each tissue sample was divided and a portion was fixed in neutral-buffered formalin for histopathology, with the remainder homogenized to yield a single cell suspension, as previously described (24). To detect any viable BCG, serial dilutions of this homogenate were plated onto 7H11 agar and incubated at 37°C, 5% CO<sub>2</sub> for three weeks. Single cell suspensions were portioned immediately for flow cytometric staining with the remainder cryopreserved in RPMI 1640/FBS containing 10% DMSO in liquid nitrogen. Formalin-fixed tissue was embedded in paraffin, sectioned, and stained with hematoxylin and eosin for microscopic examination.

### **SIV plasma viremia:**

The number of SIV RNA copies per milliliter was measured using a two-step real-time qPCR assay. Viral RNA was extracted from 500 µL of plasma using an automated sample preparation platform QIAasympy SP (Qiagen, Hilden, Germany), along with a Virus/Pathogen DSP midi kit and the *cellfree500* protocol (Qiagen). The extracted RNA was annealed to a reverse primer specific to the gag gene of SIVmac239 (5'-CAC TAG GTG TCT CTG CAC TAT CTG TTT TG -3'), then reverse transcribed to obtain cDNA using SuperScript<sup>TM</sup> III Reverse Transcriptase (Thermo Fisher Scientific, Waltham, MA) along with RNase Out. The resulting cDNA was treated with RNase H and combined with a custom 4x TaqMan<sup>TM</sup> Gene Expression Master Mix (Thermo Fisher Scientific) containing primers and a fluorescently labeled hydrolysis probe specific for the gag gene of SIVmac239 (forward primer 5'-GTC TGC GTC ATC TGG TGC ATT C -3', reverse primer 5'-CAC TAG GTG TCT CTG CAC TAT CTG TTT TG -3', probe 5'-/56-FAM/CTT CCT CAG TGT GTT TCA CTT TCT CTT CTG CG/3BHQ\_1/-3'). The qPCR was performed using a StepOnePlus<sup>TM</sup> or QuantStudio 3 Real-Time PCR System (Thermo Fisher Scientific). To determine the SIV gag RNA copies per reaction, quantification cycle data and a serial dilution of a well-characterized custom RNA transcript containing a 730 bp sequence of the SIV gag gene were used. The mean RNA copies per mL were calculated by adjusting for the dilution factor. The limit of quantification (LOQ) was determined based on the exact binomial confidence boundaries and the percent detection of the target RNA concentration, which is approximately 62 copies per mL.

### **Multiparameter flow cytometry:**

Cells from BAL, PBMC, and tissue collected at necropsy were stained for flow cytometric analysis. BAL and necropsy tissue were stained promptly upon collection, while cryopreserved PBMC were stained as a batch. Cells were seeded at  $1 \times 10^6$  cells/well in a 96-well plate in ELISpot media, then stimulated with either Mtb H37Rv whole cell lysate (WCL, 20 µL/mL; BEI Resources) or PDBu and ionomycin (P&I) for 6 hours at 37°C. After 2 hours of incubation, Golgi Plug (BD Biosciences, Cat no. 555029) was added at 8 µg/mL,

incubated for an additional 4 hours, and washed twice with PBS. Live/Dead stain was added and incubated for 10 minutes at room temperature in the dark, then washed twice with PBS. A cocktail of the surface stain (Supplemental Table 1) supplemented with BD Horizon™ Brilliant Stain buffer (BD Biosciences, Cat no. 566349) was added to each well (50 µL/well). After 20 minutes of incubation at 4°C, the cells were washed twice and permeabilized for intracellular staining (ICS) with BD Cytofix/Cytoperm™ (BD Biosciences, Cat no. 554722) for 10 minutes at room temperature. For intranuclear staining (INS) of transcription factors (necropsy samples only), 1x True-Nuclear™ (BD Biosciences, Cat. No. 424401) was added and incubated for 45 minutes. The cells were then washed twice with 1x perm wash for ICS or True-Nuclear™ 1x Fix Perm wash buffer for INS. Staining was done with 50 µL/well of the ICS and INS antibody cocktails (Supplemental Table 1) for 20 and 30 minutes, respectively. This was followed by washing twice and resuspending the stained cells in 150 µL of FACs buffer. Samples were run on a BD Cytex Aurora and analyzed using FlowJo Software for Mac OS (v10.8.1). Detailed gating strategies are shown in Supplemental Figure 3a–d.

### Plasma and BAL antibody ELISA:

Plasma and 10–12 fold concentrated BALF were used to measure IgG and IgM titers to Mtb H37Rv WCL and lipoarabinomannan (LAM), as previously described (16). Briefly, 1 µg of WCL and LAM were coated onto 96-well Costar® Assay plate (Nunc). Coated plates were blocked with PBS/10% FBS for two hours at room temperature and washed with PBS/0.05% Tween 20. Concentrated BALF or plasma 1:5 serially diluted (8 dilutions/sample) were then incubated for two hours at 37 °C and washed. Then 100 µL/well of HRP-conjugated goat anti-monkey IgG h+l (50 ng/ml; Bethyl Laboratories, Inc.), or IgM chain (0.1 µg/ml; Rockland Immunochemicals Inc.) was added and the plates incubated for 2 hours at room temperature. Plates were developed with 100 µL/well Ultra TMB® substrate (Invitrogen) and fixed with 100 µL/well 2N sulfuric acid. Plates were read at 450 nm using a Spectramax190 microplate reader (Molecular Devices) and presented as endpoint titers for IgG or midpoint titers for IgM when samples did not titer to a cut-off. Endpoint titers are reported as the reciprocal of the last dilution with an optical density (OD) above the detection limit or twice the OD of an empty well.

### Statistical analysis:

All the data were transformed as  $\log_{10}(x + 1)$ . Longitudinal BAL, PBMC, and SIV viremia data were analyzed using a mixed model fit using the Restricted Maximum Likelihood (REML) with the Geisser-Greenhouse correction. Individual animals were considered a random variable. Fixed effect tests were used to evaluate the differences between different time points, vaccine route, or vaccine route versus time points. All results from pairwise comparisons of interest (comparisons among time points within vaccine group and comparison between IV BCG vs ID BCG within time points) were reported as uncorrected Fisher's Least Significant Difference (LSD) p-values. Shapiro-Wilk test was used to test data for normality. Comparisons between IV BCG and ID BCG were made using the unpaired t-test for normally distributed data or the Mann-Whitney test for nonparametric data. Bivariate relationships were assessed using Pearson's correlation coefficient (r). All tests conducted in the study were two-sided, and statistical significance was determined at a



significance level of  $P < 0.05$ .  $P$ -values ranging from 0.05 to 0.10 were deemed indicative of a trend. GraphPad Prism 10 for MacOS (Version 10.0.2) was used for statistical analyses.

## Results

### IV BCG transiently increases plasma SIV viremia.

The study was designed to compare immune responses to IV or ID BCG in SIV-infected MCM without the confounding variable of Mtb challenge. Animals were infected with 3,000 TCID<sub>50</sub> SIVmac239 for 16 weeks and then randomized into two groups to be vaccinated with BCG by either the IV route (n=5) or the ID (n=6) route (Figure 1a). Animals in the IV BCG group were treated for two months with HRE, an anti-BCG drug combination, starting 3 weeks after vaccination to reduce the risk of BCGosis in these immunocompromised animals (19). We cultured blood samples at 1, 2, and 4 weeks, and BALF at 4 weeks after vaccination. Viable BCG was detected only in the blood of IV-vaccinated MCM one and two weeks post-BCG, and no culturable BCG was found in any BAL sample. Plasma viremia peaked within 2 weeks of SIV infection, then spontaneously fell to the viral set-point unique to each animal (Figure 1b). Animals with plasma viremia set points above 10<sup>5</sup> copies/ml were considered to be “non-controllers”, indicating an inability to naturally control SIV replication (35–37). Two animals in each vaccination group were non-controllers by 14 weeks post-SIV infection (pre-BCG) (Figure 1b, non-controllers marked with star symbols). The median viremia at 14 weeks (pre-vaccination) was higher in the IV BCG group (Figure 1b, bottom panel). ID BCG vaccination did not significantly affect plasma viremia (Figure 1b, top panel), although SIV replication transiently increased in one animal 3 weeks after ID BCG. In contrast, IV BCG elicited a significant increase in plasma viremia in all animals within 2 weeks, which spontaneously returned to the approximate pre-BCG setpoints in most animals over the next 10 weeks (Figure 1b, bottom panel), as seen previously (19).

### IV BCG elicits more T cells in the airway.

Immune responses in the airway are associated with IV BCG-elicited protection against Mtb infection (16, 34). Analysis of BAL samples taken 4 and 15 weeks after SIV infection (before vaccination) revealed no significant difference in total leukocyte and T cell counts from pre-SIV levels (Figure 2a, b). However, CD4<sup>+</sup> T cells were significantly reduced and CD4<sup>+</sup>CD8α<sup>+</sup> T cells were modestly reduced 4 weeks after SIV infection in both groups, but Vγ9+γδ were significantly reduced in ID BCG group (Figure 2b). All three cell populations returned to pre-SIV levels prior to BCG vaccination, except in animals with high viremia (Figure 2b). B cells and CD11b-CD11c<sup>+</sup> (likely dendritic cells) were also significantly depleted in the ID BCG groups following SIV infection (Supplemental Figure 1a).

Following IV BCG vaccination, animals exhibited modest increases in leukocyte count and significant increases in T, B, and NK cells in the airways. These cell counts remained unchanged in the ID-vaccinated animals (Figure 2a, Supplemental Figure 1a). Notably, IV BCG, but not ID BCG, induced significant increases in CD8αβ<sup>+</sup>, CD8αα<sup>+</sup>, Vγ9+γδ, and Vγ9-γδ T cells and modest increases in CD4<sup>+</sup>, and CD4<sup>+</sup>CD8α<sup>+</sup> T cells 4 weeks after vaccination (Figure 2b, and Table 1). These cell types returned to pre-BCG levels by 18 weeks post-vaccination, except Vγ9-γδ T cells which remained elevated (Figure 2a, 2b, and

Table 1). There was no correlation between airway CD4<sup>+</sup> T cell levels with SIV viremia in either group (Data not shown). Thus, we show IV BCG but not ID BCG elicits an influx of T cells into the airway of SIV-infected MCM.

#### **IV BCG elicits more robust airway T cell responses than ID BCG.**

We evaluated the ability of CD4<sup>+</sup> and CD8 $\alpha\beta$ <sup>+</sup> T cells in the airways to produce cytokines, focusing on those involved in Th1 (IFN $\gamma$ , IL-2, TNF) and Th17 (IFN $\gamma$ , IL-2, IL-17, TNF) responses due to their important roles in TB protection (20, 38, 39). Cytokine responses were assessed after *ex vivo* restimulation with Mtb WCL to measure mycobacterial-specific responses. The number of antigen-specific CD4<sup>+</sup> T cells in the airways producing Th1- and Th17-related cytokines significantly increased 4 weeks after BCG, regardless of vaccine route (Figure 3a). Th1 CD4<sup>+</sup> T cell responses remained significantly elevated up to 18 weeks in only the IV BCG group, while Th17 responses remained elevated in both IV- and ID-vaccinated groups (Figure 3a). In contrast, only ID BCG elicited significant Th1 and Th17 responses in airway CD8 $\alpha\beta$ <sup>+</sup> T cells by 4 weeks post-vaccination. However, by 18 weeks after vaccination, Th1 and Th17 CD8 $\alpha\beta$ <sup>+</sup> T cells were significantly increased in IV-vaccinated animals, while those responses were waning in the ID-vaccinated animals (Figure 3b). In summary, BCG vaccination by both the ID and IV routes elicited cytokine responses in airway CD4<sup>+</sup> T cells by 4 weeks, but CD8 $\alpha\beta$ <sup>+</sup> T cell responses were delayed following IV BCG. IV BCG resulted in more sustained CD4<sup>+</sup> and CD8 $\alpha\beta$ <sup>+</sup> T cell responses than ID BCG.

#### **Only IV BCG induces an influx of cytotoxic CD8 $\alpha\beta$ <sup>+</sup> and NK cells in airways.**

We next evaluated production of the cytotoxic effector granzyme B (GzmB) and granzyme K (GzmK) by CD8 $\alpha\beta$ <sup>+</sup> T cells and NK cells recovered from the airways. Cytotoxic effectors may contribute to Mtb protection by lysing infected cells and/or intracellular killing of bacteria (40–42). SIV infection significantly increased both GzmB<sup>+</sup> and GzmK<sup>+</sup> CD8 $\alpha\beta$ <sup>+</sup> T cells in both groups (Figure 4a), but did not affect the number of NK cells producing granzymes (Figure 4b). Following vaccination, IV BCG, but not ID BCG, elicited an additional and significant boost in CD8 $\alpha\beta$ <sup>+</sup> T cells producing GzmB or GzmK, with GzmB<sup>+</sup> cells remaining modestly elevated 18 weeks after vaccination. IV BCG also significantly increased the number of NK cells producing either GzmB or GzmK, but returned to pre-vaccination levels 18 weeks after BCG (Figure 4b and Table 1). These data demonstrate that IV BCG induces an early influx of cytotoxic effectors from CD8 $\alpha\beta$ <sup>+</sup> T cells and NK in the airways.

#### **Transient changes in circulating immune populations following vaccination.**

PBMC were analyzed by flow cytometry to assess effects of BCG vaccination on circulating cell populations. Following SIV infection, the number of CD4<sup>+</sup> and V $\gamma$ 9<sup>+</sup> $\gamma$ 8<sup>+</sup> T cells were significantly depleted in the IV BCG and ID BCG groups, respectively, prior to vaccination (Supplemental Figure 1c). Surprisingly, IV BCG vaccination induced a significant depletion in the number of NK, B cells, CD4<sup>+</sup> and CD4<sup>+</sup>CD8 $\alpha$ <sup>+</sup> T cells by 4 weeks post-vaccination, while V $\gamma$ 9<sup>+</sup> $\gamma$ 8<sup>+</sup> T cells were depleted 4 weeks after ID BCG vaccination. These cell types returned to their pre-BCG levels by 18 weeks post-vaccination,



although a significant decrease in NK cells remained at this late time point in ID-vaccinated animals (Supplemental Figure 1b, 1c).

#### **IV BCG induces mycobacterial-specific antibody response in plasma and airways.**

We used ELISAs to measure WCL- and LAM-specific antibodies in plasma and BALF after BCG vaccination. IgG and IgM levels were associated with Mtb protection in IV BCG-vaccinated macaques (16, 19, 21, 43). Here, we observed a significant increase in plasma IgG specific for WCL and LAM following both ID and IV BCG by 4 weeks (Figure 5a, top panels). However, LAM-specific IgG in plasma returned to pre-BCG levels in both IV and ID BCG-vaccinated MCM by 18 weeks post-vaccination, while WCL-specific IgG returned to pre-BCG levels only in the ID BCG-vaccinated group (Figure 5a). Both IV and ID BCG elicited significant WCL-specific IgM in plasma, but only IV BCG induced significant LAM-specific IgM 4 weeks post-vaccination (Figure 5a, bottom panels). By 18 weeks after BCG, the IgM responses remained significant in the IV- compared to the ID BCG-vaccinated group (Figure 5a, Table 2).

In airways, IV BCG, but not ID BCG, elicited a significant increase in WCL-specific IgG and IgM while LAM-specific IgG and IgM responses were significant in both IV and ID BCG 4 weeks after vaccination (Figure 5b). However, both WCL- and LAM-specific antibodies declined to pre-BCG levels by 18 weeks after vaccination. (Figure 5b). Comparing each time point between IV and ID BCG showed that IV BCG elicited higher levels of LAM- and WCL-specific IgG in the airways at 4 weeks post-BCG than ID BCG. However, by 18 weeks after BCG vaccination, only LAM-specific IgG and IgM were significant in the airway of IV compared to ID BCG-vaccinated group (Table 2).

#### **IV BCG induces robust immune responses in lung tissue.**

We interrogated immune responses across various tissues in BCG-vaccinated SIV+ MCM without the confounding variable of Mtb challenge, something that was not possible in our previous study in which all SIV+, BCG-vaccinated animals underwent Mtb challenge (19). Here, we conducted necropsies 5 months after vaccination, without Mtb challenge. Samples from lung, lymph nodes, and spleen were plated on agar to detect any viable BCG. We did observe one bacterial colony in a lung sample from a single IV-vaccinated animal in the HRE treatment group, which was confirmed by PCR to be BCG. Since no BCG was cultured from any other HRE-treated animal, and since this animal yielded just a single colony, the HRE regimen was largely effective.

We compared T cell responses in lungs, thoracic lymph nodes, and spleen five months after vaccination. Since  $T_{RM}$  cells were associated with IV BCG-elicited protection (16), we included anti-CD69 antibody, a canonical marker of  $T_{RM}$  cells and activation (33, 44) in our flow panels (Supplemental Table 1). To differentiate  $T_{RM}$  immune cells from those in circulation, fluorescently-labeled anti-CD45 antibody was administered just prior to euthanasia (16, 34). Thus, tissue-resident cells (anti-CD45 negative) can be differentiated from bloodborne cells (anti-CD45 positive). We designated the CD69+ivCD45- population to be  $T_{RM}$  cells (Fig. 6a), although this strategy may also mischaracterize some activated T cells as well. This analysis revealed significantly more  $T_{RM}$  cells in lungs of animals that

received IV BCG compared to ID BCG (Figure 6a and 6b). Of the other T<sub>RM</sub> cell subsets identified, there were significantly more CD8 $\alpha$  $\beta$ <sup>+</sup>, CD8 $\alpha$  $\alpha$ <sup>+</sup>, and  $\gamma$  $\delta$ <sup>+</sup> T cells in lung tissue of IV BCG-vaccinated animals (Figure 6c). CD4<sup>+</sup> and CD4<sup>+</sup>CD8 $\alpha$ <sup>+</sup> T cell numbers did not differ significantly between the groups, most likely due to the low CD4<sup>+</sup> T cell numbers in the MCM with higher SIV viral levels (Figure 6c). Indeed, CD4<sup>+</sup> T cells in lung were modestly inversely correlated with SIV plasma viremia in both ID and IV BCG MCM (Data not shown). T<sub>RM</sub> cell subset numbers in thoracic lymph node were similar in animals vaccinated with either ID or IV BCG (Supplemental Figure 2a), and the number of CD4<sup>+</sup> and CD4<sup>+</sup>CD8 $\alpha$ <sup>+</sup> T cells in thoracic lymph nodes appeared independent of SIV viremia level (Supplemental Figure 2a).

#### **IV BCG may induce more CD4<sup>+</sup> T cell cytokines but not CD8 $\alpha$ $\beta$ <sup>+</sup> T cells and NK cells cytotoxic effectors in lung tissue.**

We stimulated lung, thoracic lymph nodes, and spleen with WCL to assess production of cytokines associated with Th1 (IFN $\gamma$ , IL-2, TNF) and Th17 (IFN $\gamma$ , IL-2, IL-17, TNF) responses from CD4<sup>+</sup> and CD8 $\alpha$  $\beta$ <sup>+</sup> T cells. The number of CD4<sup>+</sup> T cells producing a combination of Th1- and Th17-associated cytokines in the lung were higher in animals vaccinated via IV BCG than ID BCG, but not in the thoracic lymph node (Figure 7a, 7b, and Supplemental Figure 2b, 2c). MCM with high SIV viremia had lower numbers of responding CD4<sup>+</sup> T cells. CD8 $\alpha$  $\beta$ <sup>+</sup> T cells from all three sites produced some combination of Th1 and Th17 cytokines at similar levels in both IV- and ID-vaccinated animals (Figure 7a, 7b, and Supplemental Figure 2b, 2c).

We measured the number of CD8 $\alpha$  $\beta$ <sup>+</sup> T cells and NK cells producing granulysin, GzmB, GzmK, or perforin in lung, thoracic lymph nodes, and spleen. Our data revealed similar numbers of CD8 $\alpha$  $\beta$ <sup>+</sup> T cells and NK cells producing these cytotoxic effectors in lung and thoracic lymph nodes regardless of vaccination group (Supplemental Figure 2d–g). In the spleen, there were significantly more CD8 $\alpha$  $\beta$ <sup>+</sup> T cells producing GzmK and a trend towards more CD8 $\alpha$  $\beta$ <sup>+</sup> T cells producing GzmB in IV- than ID-vaccinated animals (Data not shown), but NK cells producing cytotoxic effector show no significant difference in number in all the tissues (Supplemental Figure 2d–g).

There was no apparent effect of plasma SIV viremia on granulysin-, GzmB-, GzmK-, or perforin-producing CD8 $\alpha$  $\beta$ <sup>+</sup> T cells in the lung. However, spleens of IV BCG animals with higher plasma SIV viremia had the lowest GzmB-, GzmK-, or perforin-producing NK cells (Data not shown).

The transcription factors Foxp3, ROR $\gamma$ T, and T-bet are associated with regulatory T cells, Th17 cells, and Th1 cells, respectively (45, 46). The number of CD4<sup>+</sup> and CD8 $\alpha$  $\beta$ <sup>+</sup> T cells expressing Foxp3, ROR $\gamma$ T, or T-bet did not differ in lung, thoracic lymph node, or spleen between animals vaccinated by the IV or ID route (Data not shown).

In summary, our data show that IV BCG induces robust and sustained T helper and cytotoxic T cell response in the airways of SIV<sup>+</sup> MCM. Notably, even 5 months after vaccination, IV BCG-vaccinated animals had higher numbers of T<sub>RM</sub> cells in the lungs compared to ID BCG-vaccinated animals.

## Discussion:

PLWH are at increased risk from Mtb and a safe, effective TB vaccine for this population would be enormously beneficial. In SIV-naïve rhesus macaques, IV BCG vaccination provided superior protection from TB compared to ID BCG and correlated with mycobacterial-specific T cells in the airways and T<sub>RM</sub> cells in lung tissue, mycobacterial-specific antibodies, and distinct transcriptional signatures (16, 20, 21, 47). We recently showed that IV BCG was also highly protective in MCM with preexisting SIV infection (19). Fully characterizing the immune responses induced by IV BCG in SIV+ MCM is important to further develop or learn from this vaccine strategy. However, it is difficult to differentiate immune responses in tissues induced by BCG from those induced by Mtb after vaccinated MCM are challenged with Mtb. Here, we investigated cellular and humoral immune responses to IV BCG in SIV-infected MCM in the blood, airways, and tissues without the confounding factor of Mtb challenge. We compared those to the responses induced by ID BCG in SIV-infected MCM as this route is used currently to vaccinate against TB. Our data demonstrate that in many ways the two vaccination routes induce similar immune responses in SIV+ MCM, but several features were unique to IV BCG-vaccinated animals, including some not investigated previously.

In our previous work using SIV-naïve rhesus macaques, IV BCG induced a robust T cell influx into airways, especially CD4+, CD8αβ+, and nonconventional (Vγ9+γδ and MAIT) T cells (16). We also showed a significant influx of these T cell subsets in SIV+ MCM after IV BCG vaccination (19). Here, we directly compared IV and ID BCG in SIV+ MCM and observed more CD4+ and CD8αβ+ T cells in airways following IV vaccination. We also detected an increased influx of Vγ9+ and Vγ9-γδ T cells into the airway following IV but not ID BCG as seen previously in SIV-naïve rhesus macaques (16, 48). We noted that more B and NK cells accumulated in the airways of the IV BCG-vaccinated, SIV-infected MCM. This is consistent with our previous study in SIV+ MCM (19) as well as our study in SIV-naïve rhesus macaques (16). The latter study is particularly notable as the number of NK cells in the airways correlated with IV BCG-induced protection from Mtb (20). Thus, a key feature that differentiates IV BCG from ID BCG is a significant influx into airways of diverse lymphocyte populations which have all been shown to be associated with controlling Mtb in humans (49).

We also assessed the functionality of the cells that migrated to the airways in response to IV or ID vaccination. Both routes induced polyfunctional CD4+ T cells that produced Th1- and Th17-associated cytokines by 4 weeks. However, this response was more sustained in IV BCG-vaccinated animals, with significant elevation over 5 months. Polyfunctional T cells correlate with protection or improved outcome from Mtb in both humans and NHP (16, 20, 50–52), and we previously reported their induction following IV BCG vaccination in SIV+ MCM (19). In particular, Th1 and Th17 cytokines response elicited by BCG delivered via IV (20,53) or intrabronchially (38) have been associated with protection from Mtb. We showed here that CD8αβ+ T cell producing Th1- and Th17-related cytokines appeared in airways by 4 weeks after ID BCG but then waned over time. In contrast, Th1- and Th17- CD8αβ+ T cells were initially low following IV BCG but increased significantly by 18 weeks post-vaccination. Further, only IV BCG boosted the number of NK and

CD8 $\alpha\beta$ + T cells producing either GzmB or GzmK cytotoxic effector which had not been previously investigated. The protective efficacy of IV BCG may be related to the quality of the lymphocytes in the airways as well as the durability of those responses following vaccination.

Previous studies have shown that Mtb-specific antibody is associated with BCG-induced protection against Mtb in both SIV+ and SIV-naïve macaque (16, 19, 20, 53). Here, we demonstrated that IV BCG induces higher levels of mycobacterial-specific IgG and IgM in both the airways and plasma of SIV+ MCM than ID BCG. These antibodies were higher 4 weeks after vaccination than 18 weeks after vaccination and followed the kinetics of the B cells recovered from BAL. We previously reported increased mycobacterial-specific antibodies in both BAL and plasma from SIV+ MCM 12 weeks after IV BCG but did not assess other post-vaccination time points (19). These current results suggest that IV BCG recruits B cells to the airways and induces a robust IgG and IgM response a few weeks after vaccination which then subside. While it is likely that these antibody responses are a result of the increased number of B cells following IV vaccination, we cannot exclude other contributing factors such as the higher BCG IV dose. Since IV BCG-elicited IgM is associated with protection in rhesus macaques (21), it is likely that this humoral response remains primed to react quickly to Mtb challenge.

T<sub>RM</sub> cells in the lung have been associated with protection from TB in mice (54) as well as in IV BCG-vaccinated rhesus macaques (16). In our previous study of IV BCG in SIV+ MCM (19), all animals underwent Mtb challenge and so we could not characterize vaccine-associated immune responses within tissues. The design of the current study did not include Mtb challenge and made it possible to evaluate T<sub>RM</sub> cells within tissues in response to ID and IV BCG in SIV+ MCM. The use of intravascular anti-CD45 antibody (34) ensured that we analyzed tissue-resident, rather than circulating, immune cells. Our data revealed that even at 5 months post-vaccination, there were significantly more T<sub>RM</sub> cells in lungs of SIV+ IV BCG-vaccinated MCM, compared to those vaccinated ID. These T<sub>RM</sub> cells consisted of diverse T cell subsets, including CD4+, CD8 $\alpha\beta$ +, CD8 $\alpha\alpha$ +, CD4+CD8 $\alpha$ +, and  $\gamma\delta$ +. This finding is consistent with our previous study conducted in SIV-naïve macaques, which demonstrated more T<sub>RM</sub> in lungs of macaques vaccinated with IV BCG compared to aerosol or ID routes (16). Studies in mice also have shown that intranasal vaccination leads to greater accumulation of T<sub>RM</sub> in the lungs compared to ID vaccination (54). Higher lung T<sub>RM</sub> numbers elicited by IN BCG also correlated with better protection from Mtb in mice (55). In contrast, the number of T<sub>RM</sub> cells in thoracic lymph nodes and spleen were similar between ID- and IV-vaccinated MCM, suggesting that IV BCG selectively promotes the accumulation and retention of T cells in lung tissue. Interestingly, the production of Th1 and Th17 cytokines, cytotoxic molecules, and transcription factors by these lung T cells did not differ between MCM vaccinated with ID or IV BCG, although the number of cells producing these effectors was increased in IV-vaccinated animals. These data suggest that IV BCG confers protection, at least in part, by increasing the number of mycobacteria-specific T<sub>RM</sub> cells in the lung rather than by inducing unique T cell responses. We previously showed a high numbers of polyfunctional CD4+ and CD8 $\alpha\beta$ + T cell in lungs of SIV-naïve rhesus macaques 4 weeks after IV BCG than aerosol and ID BCG vaccination (16). It is notable that, here, we evaluated lung-resident T cells 5 months post-BCG and observed

higher numbers in IV BCG-vaccinated SIV+ animals which suggests that the increase in lung T<sub>RM</sub> cells following IV BCG is quite durable. We speculate that IV BCG results in extensive T cell priming in lymph nodes and spleen and promotes their recruitment and retention in the lung, perhaps due to the persistence of BCG antigens following IV vaccination. This is supported by our previous finding in SIV-naïve rhesus macaques that viable BCG, albeit in low numbers, could be cultured from more organs 1 month after vaccination by the IV route compared to the ID route (16).

SIV plasma viremia peaked shortly after SIV infection, which coincided with the depletion of CD4+ T cells and CD4+CD8α+ T cells, consistent with findings from our previous study and others (19, 56). We also noted depletion of Vγ9+γδ T cells in both the blood and airways at this same time, which is in line with reports of early depletion of circulating Vγ9+γδ T cells in HIV-infected people (57–59). Although the reason for Vγ9+γδ T cell depletion remains unclear, we speculate that it may be related to the high level of CCR5, an SIV coreceptor, on these cells.

IV BCG induced a transient spike in SIV viremia following vaccination, as we reported previously (19). However, the current study was limited by a larger-than-expected number of animals with persistently high SIV viremia. Although the four non-controllers were distributed evenly between both experimental groups, it limited our ability to compare rigorously the immune responses in animals vaccinated by the IV and ID routes. These SIV non-controllers exhibited low numbers of CD4+ and CD4+CD8α+ T cells in blood and BAL as we seen previously (19, 25). These animals also had fewer CD4+ T<sub>RM</sub> cells in lung tissue. Other cell types and antibody responses appeared unaffected by SIV viral loads. MCM with higher SIV loads were not protected from Mtb challenge (19), suggesting a detrimental effect of high viremia on the protective efficacy of IV BCG. Consequently, only three of five IV-vaccinated animals exhibited SIV control in our current study and, based on previous data (19), would have been likely to prevent TB.

In summary, the data presented here demonstrate clearly that BCG delivered to SIV+ MCM by the IV route leads to significantly higher numbers of lymphocyte populations in the airways, higher levels of mycobacterial-specific IgG and IgM, and more T<sub>RM</sub> cells in the lung compared to ID vaccination. These findings inform potential mechanisms underlying the protection conferred by IV BCG in SIV+ MCM and provide valuable insights into vaccine design for PLWH.

## Supplementary Material

Refer to Web version on PubMed Central for supplementary material.

## Acknowledgements:

We are very grateful to the veterinary, laboratory, and analytical teams in the TB Research Group at the University of Pittsburgh for their dedicated work. We also thank Drs. Robert Seder and Patricia Darrah (VRC, NIAID, NIH) for helpful discussions.

This work was funded by NIH R01 AI155345 (Scanga). Dr. Erica Larson was supported by NIH K01 OD033539. SIV assays were supported by the NIH NIAID DAIDS Nonhuman Primate Core Virology Laboratory for AIDS Vaccine Research and Development Contract # HHSN272201800003C (DeMarco). Award P51OD011107 from



the Office of Research Infrastructure Program, NIH supports the Primate Assay Laboratory of the California National Primate Research Center, which supplied the SIVmac239. Award UC7A1180311 from NIAID supports the operation of The University of Pittsburgh Regional Biocontainment Laboratory (RBL) within the Center for Vaccine Research (CVR).

## References:

1. WHO. 2022. Global tuberculosis report 2022. Geneva: World Health Organization.
2. WHO. 2021. Global TB Report 2021 Geneva: World Health Organization.
3. Miner MD, Hatherill M, Mave V, Gray GE, Nachman S, Read SW, White RG, Hesselning A, Cobelens F, and Patel S. 2022. Developing tuberculosis vaccines for people with HIV: consensus statements from an international expert panel. *The Lancet HIV*.
4. Geldmacher C, Zumla A, and Hoelscher M. 2012. Interaction between HIV and Mycobacterium tuberculosis: HIV-1-induced CD4 T-cell depletion and the development of active tuberculosis. *Curr Opin HIV AIDS* 7: 268–275. [PubMed: 22495739]
5. Amelio P, Portevin D, Hella J, Reither K, Kamwela L, Lweno O, Tumbo A, Geoffrey L, Ohmiti K, Ding S, Pantaleo G, Daubenberger C, and Perreau M. 2019. HIV Infection Functionally Impairs Mycobacterium tuberculosis-Specific CD4 and CD8 T-Cell Responses. *J Virol* 93.
6. Esmail H, Riou C, du Bruyn E, Lai RP-J, Harley YX, Meintjes G, Wilkinson KA, and Wilkinson RJ. 2018. The immune response to Mycobacterium tuberculosis in HIV-1-coinfected persons. *Annual review of immunology* 36: 603–638.
7. Zhang L, Jiang X, Pfau D, Ling Y, and Nathan CF. 2021. Type I interferon signaling mediates Mycobacterium tuberculosis-induced macrophage death. *Journal of Experimental Medicine* 218.
8. Sandler NG, Bosinger SE, Estes JD, Zhu RTR, Tharp GK, Boritz E, Levin D, Wijeyesinghe S, Makamdop KN, del Prete GQ, Hill BJ, Timmer JK, Reiss E, Yarden G, Darko S, Contijoch E, Todd JP, Silvestri G, Nason M, Norgren RB Jr, Keele BF, Rao S, Langer JA, Lifson JD, Schreiber G, and Douek DC. 2014. Type I interferon responses in rhesus macaques prevent SIV infection and slow disease progression. *Nature* 511: 601–605. [PubMed: 25043006]
9. Li Y, and Sun W. 2018. Effects of Th17/Treg cell imbalance on HIV replication in patients with AIDS complicated with tuberculosis. *Experimental and Therapeutic Medicine* 15: 2879–2883. [PubMed: 29456692]
10. Kaw S, Ananth S, Tsopoulidis N, Morath K, Coban BM, Hohenberger R, Bulut OC, Klein F, Stolp B, and Fackler OT. 2020. HIV-1 infection of CD4 T cells impairs antigen-specific B cell function. *Embo j* 39: e105594. [PubMed: 33146906]
11. Larson EC, Ellis-Connell A, Rodgers MA, Balgeman AJ, Moriarty RV, Ameel CL, Baranowski TM, Tomko JA, Causgrove CM, Maiello P, O'Connor SL, and Scanga CA. 2021. Pre-existing Simian Immunodeficiency Virus Infection Increases Expression of T Cell Markers Associated with Activation during Early Mycobacterium tuberculosis Coinfection and Impairs TNF Responses in Granulomas. *J Immunol* 207: 175–188. [PubMed: 34145063]
12. Wong K, Nguyen J, Blair L, Banjanin M, Grewal B, Bowman S, Boyd H, Gerstner G, Cho HJ, Panfilov D, Tam CK, Aguilar D, and Venketaraman V. 2020. Pathogenesis of Human Immunodeficiency Virus-Mycobacterium tuberculosis Co-Infection. *J Clin Med* 9.
13. Nemes E, Geldenhuys H, Rozot V, Rutkowski KT, Ratangee F, Bilek N, Mabwe S, Makhethle L, Erasmus M, and Toefy A. 2018. Prevention of M. tuberculosis infection with H4: IC31 vaccine or BCG revaccination. *New England Journal of Medicine* 379: 138–149. [PubMed: 29996082]
14. Tait DR, Hatherill M, Van Der Meeren O, Ginsberg AM, Van Brakel E, Salaun B, Scriba TJ, Akite EJ, Ayles HM, Bollaerts A, Demoitie MA, Diacon A, Evans TG, Gillard P, Hellström E, Innes JC, Lempicki M, Malahleha M, Martinson N, Mesia Vela D, Muyoyeta M, Nduba V, Pascal TG, Tameris M, Thienemann F, Wilkinson RJ, and Roman F. 2019. Final Analysis of a Trial of M72/AS01(E) Vaccine to Prevent Tuberculosis. *N Engl J Med* 381: 2429–2439. [PubMed: 31661198]
15. Darrah PA, DiFazio RM, Maiello P, Gideon HP, Myers AJ, Rodgers MA, Hackney JA, Lindstrom T, Evans T, Scanga CA, Prikhodko V, Andersen P, Lin PL, Laddy D, Roederer M, Seder RA, and Flynn JL. 2019. Boosting BCG with proteins or rAd5 does not enhance protection against tuberculosis in rhesus macaques. *NPJ Vaccines* 4: 21. [PubMed: 31149352]



16. Darrah PA, Zeppa JJ, Maiello P, Hackney JA, Wadsworth MH 2nd, Hughes TK, Pokkali S, Swanson PA 2nd, Grant NL, Rodgers MA, Kamath M, Causgrove CM, Laddy DJ, Bonavia A, Casimiro D, Lin PL, Klein E, White AG, Scanga CA, Shalek AK, Roederer M, Flynn JL, and Seder RA. 2020. Prevention of tuberculosis in macaques after intravenous BCG immunization. *Nature* 577: 95–102. [PubMed: 31894150]
17. Hesselting AC, Marais BJ, Gie RP, Schaaf HS, Fine PE, Godfrey-Faussett P, and Beyers N. 2007. The risk of disseminated Bacille Calmette-Guerin (BCG) disease in HIV-infected children. *Vaccine* 25: 14–18. [PubMed: 16959383]
18. World Health O 2018. BCG vaccine: WHO position paper, February 2018 - Recommendations. *Vaccine* 36: 3408–3410. [PubMed: 29609965]
19. Larson EC, Ellis-Connell AL, Rodgers MA, Gubernat AK, Gleim JL, Moriarty RV, Balgeman AJ, Ameel CL, Jauro S, Tomko JA, Kracinovsky KB, Maiello P, Borish HJ, White AG, Klein E, Bucsán AN, Darrah PA, Seder RA, Roederer M, Lin PL, Flynn JL, O'Connor SL, and Scanga CA. 2023. Intravenous Bacille Calmette–Guérin vaccination protects simian immunodeficiency virus-infected macaques from tuberculosis. *Nature Microbiology*.
20. Darrah PA, Zeppa JJ, Wang C, Irvine EB, Bucsán AN, Rodgers MA, Pokkali S, Hackney JA, Kamath M, and White AG. 2023. Airway T cells are a correlate of iv Bacille Calmette-Guerin-mediated protection against tuberculosis in rhesus macaques. *Cell Host & Microbe*.
21. Irvine EB, O'Neil A, Darrah PA, Shin S, Choudhary A, Li W, Honnen W, Mehra S, Kaushal D, Gideon HP, Flynn JL, Roederer M, Seder RA, Pinter A, Fortune S, and Alter G. 2021. Robust IgM responses following intravenous vaccination with Bacille Calmette-Guérin associate with prevention of Mycobacterium tuberculosis infection in macaques. *Nat Immunol* 22: 1515–1523. [PubMed: 34811542]
22. Liu YE, Darrah PA, Zeppa JJ, Kamath M, Laboune F, Douek DC, Maiello P, Roederer M, Flynn JL, Seder RA, and Khatri P. 2023. Blood transcriptional correlates of BCG-induced protection against tuberculosis in rhesus macaques. *Cell Rep Med* 4: 101096. [PubMed: 37390827]
23. Aandahl EM, Michaëlsson J, Moretto WJ, Hecht FM, and Nixon DF. 2004. Human CD4+ CD25+ regulatory T cells control T-cell responses to human immunodeficiency virus and cytomegalovirus antigens. *J Virol* 78: 2454–2459. [PubMed: 14963140]
24. Maiello P, DiFazio RM, Cadena AM, Rodgers MA, Lin PL, Scanga CA, and Flynn JL. 2018. Rhesus Macaques Are More Susceptible to Progressive Tuberculosis than Cynomolgus Macaques: a Quantitative Comparison. *Infect Immun* 86.
25. Larson EC, Ellis-Connell A, Rodgers MA, Balgeman AJ, Moriarty RV, Ameel CL, Baranowski TM, Tomko JA, Causgrove CM, and Maiello P. 2021. Pre-existing Simian immunodeficiency virus infection increases expression of T cell markers associated with activation during early Mycobacterium tuberculosis coinfection and impairs TNF responses in granulomas. *The Journal of Immunology* 207: 175–188. [PubMed: 34145063]
26. Moriarty RV, Rodgers MA, Ellis AL, Balgeman AJ, Larson EC, Hopkins F, Chase MR, Maiello P, Fortune SM, and Scanga CA. 2022. Spontaneous Control of SIV Replication Does Not Prevent T Cell Dysregulation and Bacterial Dissemination in Animals Co-Infected with M. tuberculosis. *Microbiology Spectrum*: e01724–01721.
27. Rodgers MA, Ameel C, Ellis-Connell AL, Balgeman AJ, Maiello P, Barry GL, Friedrich TC, Klein E, O'Connor SL, and Scanga CA. 2018. Preexisting simian immunodeficiency virus infection increases susceptibility to tuberculosis in Mauritian cynomolgus macaques. *Infection and immunity* 86: e00565–00518. [PubMed: 30224552]
28. Ellis-Connell AL, Kannal NM, Balgeman AJ, and O'Connor SL. 2019. Characterization of major histocompatibility complex-related molecule 1 sequence variants in non-human primates. *Immunogenetics* 71: 109–121. [PubMed: 30353260]
29. Fitzpatrick M, Ho MM, Clark S, Dagg B, Khatri B, Lanni F, Williams A, Brennan M, Laddy D, and Walker B. 2019. Comparison of pellicle and shake flask-grown BCG strains by quality control assays and protection studies. *Tuberculosis (Edinb)* 114: 47–53. [PubMed: 30711157]
30. Hartman AL, Nambulli S, McMillen CM, White AG, Tilston-Lunel NL, Albe JR, Cottle E, Dunn MD, Frye LJ, Gilliland TH, Olsen EL, O'Malley KJ, Schwarz MM, Tomko JA, Walker RC, Xia M, Hartman MS, Klein E, Scanga CA, Flynn JL, Klimstra WB, McElroy AK, Reed DS, and Duprex WP. 2020. SARS-CoV-2 infection of African green monkeys results in mild respiratory

disease discernible by PET/CT imaging and shedding of infectious virus from both respiratory and gastrointestinal tracts. *PLoS Pathog* 16: e1008903. [PubMed: 32946524]

31. Sarnyai Z, Nagy K, Patay G, Molnár M, Rosenqvist G, Tóth M, Takano A, Gulyás B, Major P, Halldin C, and Varrone A. 2019. Performance Evaluation of a High-Resolution Nonhuman Primate PET/CT System. *J Nucl Med* 60: 1818–1824. [PubMed: 31302634]
32. White AG, Maiello P, Coleman MT, Tomko JA, Frye LJ, Scanga CA, Lin PL, and Flynn JL. 2017. Analysis of 18FDG PET/CT Imaging as a Tool for Studying *Mycobacterium tuberculosis* Infection and Treatment in Non-human Primates. *J Vis Exp*.
33. Kauffman KD, Sallin MA, Sakai S, Kamenyeva O, Kabat J, Weiner D, Sutphin M, Schimel D, Via L, Barry CE 3rd, Wilder-Kofie T, Moore I, Moore R, and Barber DL. 2018. Defective positioning in granulomas but not lung-homing limits CD4 T-cell interactions with *Mycobacterium tuberculosis*-infected macrophages in rhesus macaques. *Mucosal Immunol* 11: 462–473. [PubMed: 28745326]
34. Potter EL, Gideon HP, Tkachev V, Fabozzi G, Chassiakos A, Petrovas C, Darrah PA, Lin PL, Foulds KE, and Kean LS. 2021. Measurement of leukocyte trafficking kinetics in macaques by serial intravascular staining. *Science Translational Medicine* 13: eabb4582.
35. Gonzalo-Gil E, Ikediobi U, and Sutton RE. 2017. Focus: Infectious diseases: Mechanisms of virologic control and clinical characteristics of HIV+ elite/viremic controllers. *The Yale journal of biology and medicine* 90: 245. [PubMed: 28656011]
36. Tetali S, Bakshi S, Than S, Pahwa S, Abrams E, Romano J, and Pahwa S. 1998. Plasma virus load evaluation in relation to disease progression in HIV-infected children. *AIDS research and human retroviruses* 14: 571–577. [PubMed: 9591711]
37. Smith SM, Holland B, Russo C, Dailey PJ, Marx PA, and Connor RI. 1999. Retrospective analysis of viral load and SIV antibody responses in rhesus macaques infected with pathogenic SIV: predictive value for disease progression. *AIDS research and human retroviruses* 15: 1691–1701. [PubMed: 10606092]
38. Dijkman K, Sombroek CC, Vervenne RAW, Hofman SO, Boot C, Remarque EJ, Kocken CHM, Ottenhoff THM, Kondova I, Khayum MA, Haanstra KG, Vierboom MPM, and Verreck FAW. 2019. Prevention of tuberculosis infection and disease by local BCG in repeatedly exposed rhesus macaques. *Nat Med* 25: 255–262. [PubMed: 30664782]
39. Larsen SE, Williams BD, Rais M, Coler RN, and Baldwin SL. 2022. It takes a village: the multifaceted immune response to *Mycobacterium tuberculosis* infection and vaccine-induced immunity. *Frontiers in Immunology* 13: 840225. [PubMed: 35359957]
40. Balin SJ, Pellegrini M, Klechevsky E, Won ST, Weiss DI, Choi AW, Hakimian J, Lu J, Ochoa MT, and Bloom BR. 2018. Human antimicrobial cytotoxic T lymphocytes, defined by NK receptors and antimicrobial proteins, kill intracellular bacteria. *Science immunology* 3: eaat7668.
41. Gideon HP, Hughes TK, Tzouanas CN, Wadsworth MH 2nd, Tu AA, Gierahn TM, Peters JM, Hopkins FF, Wei JR, Kummerlowe C, Grant NL, Nargan K, Phuah JY, Borish HJ, Maiello P, White AG, Winchell CG, Nyquist SK, Ganchua SKC, Myers A, Patel KV, Ameel CL, Cochran CT, Ibrahim S, Tomko JA, Frye LJ, Rosenberg JM, Shih A, Chao M, Klein E, Scanga CA, Ordovas-Montanes J, Berger B, Mattila JT, Madansein R, Love JC, Lin PL, Leslie A, Behar SM, Bryson B, Flynn JL, Fortune SM, and Shalek AK. 2022. Multimodal profiling of lung granulomas in macaques reveals cellular correlates of tuberculosis control. *Immunity* 55: 827–846.e810. [PubMed: 35483355]
42. Busch M, Herzmann C, Kallert S, Zimmermann A, Höfer C, Mayer D, Zenk SF, Muche R, Lange C, Bloom BR, Modlin RL, and Stenger S. 2016. Lipoarabinomannan-Responsive Polycytotoxic T Cells Are Associated with Protection in Human Tuberculosis. *Am J Respir Crit Care Med* 194: 345–355. [PubMed: 26882070]
43. Coppola M, Arroyo L, van Meijgaarden KE, Franken KL, Geluk A, Barrera LF, and Ottenhoff TH. 2017. Differences in IgG responses against infection phase related *Mycobacterium tuberculosis* (Mtb) specific antigens in individuals exposed or not to Mtb correlate with control of TB infection and progression. *Tuberculosis* 106: 25–32. [PubMed: 28802401]
44. Kumar BV, Ma W, Miron M, Granot T, Guyer RS, Carpenter DJ, Senda T, Sun X, Ho S-H, Lerner H, Friedman AL, Shen Y, and Farber DL. 2017. Human Tissue-Resident Memory T Cells Are

Defined by Core Transcriptional and Functional Signatures in Lymphoid and Mucosal Sites. *Cell Reports* 20: 2921–2934. [PubMed: 28930685]

45. Chen Z, Lin F, Gao Y, Li Z, Zhang J, Xing Y, Deng Z, Yao Z, Tsun A, and Li B. 2011. FOXP3 and ROR $\gamma$ t: transcriptional regulation of Treg and Th17. *Int Immunopharmacol* 11: 536–542. [PubMed: 21081189]
46. Qu Y, Li D, Xiong H, and Shi D. 2023. Transcriptional regulation on effector T cells in the pathogenesis of psoriasis. *Eur J Med Res* 28: 182. [PubMed: 37270497]
47. Peters JM, Irvine EB, Rosenberg JM, Wadsworth MH, Hughes TK, Sutton M, Nyquist SK, Bromley JD, Mondal R, and Roederer M. 2023. Protective intravenous BCG vaccination induces enhanced immune signaling in the airways. *bioRxiv*: 2023.2007. 2016.549208.
48. Morrison AL, Sarfas C, Sibley L, Williams J, Mabbutt A, Dennis MJ, Lawrence S, White AD, Bodman-Smith M, and Sharpe SA. 2023. IV BCG Vaccination and Aerosol BCG Revaccination Induce Mycobacteria-Responsive  $\gamma\delta$  T Cells Associated with Protective Efficacy against M. tb Challenge. *Vaccines (Basel)* 11.
49. Roy Chowdhury R, Vallania F, Yang Q, Lopez Angel CJ, Darboe F, Penn-Nicholson A, Rozot V, Nemes E, Malherbe ST, Ronacher K, Walzl G, Hanekom W, Davis MM, Winter J, Chen X, Scriba TJ, Khatri P, and Chien YH. 2018. A multi-cohort study of the immune factors associated with M. tuberculosis infection outcomes. *Nature* 560: 644–648. [PubMed: 30135583]
50. Larson E, Ellis-Connell A, Rodgers M, Gubernat A, Gleim J, Moriarty R, Balgeman A, Ameen C, Jauro S, and Tomko J. 2023. Vaccination with intravenous BCG protects macaques with pre-existing SIV infection from tuberculosis.
51. Qin S, Chen R, Jiang Y, Zhu H, Chen L, Chen Y, Shen M, and Lin X. 2021. Multifunctional T cell response in active pulmonary tuberculosis patients. *International Immunopharmacology* 99: 107898. [PubMed: 34333359]
52. Caccamo N, Guggino G, Joosten SA, Gelsomino G, Di Carlo P, Titone L, Galati D, Bocchino M, Matarese A, and Salerno A. 2010. Multifunctional CD4+ T cells correlate with active Mycobacterium tuberculosis infection. *European journal of immunology* 40: 2211–2220. [PubMed: 20540114]
53. Dijkman K, Sombroek CC, Vervenne RA, Hofman SO, Boot C, Remarque EJ, Kocken CH, Ottenhoff TH, Kondova I, and Khayum MA. 2019. Prevention of tuberculosis infection and disease by local BCG in repeatedly exposed rhesus macaques. *Nature medicine* 25: 255–262.
54. Sakai S, Kauffman KD, Schenkel JM, McBerry CC, Mayer-Barber KD, Masopust D, and Barber DL. 2014. Cutting edge: control of Mycobacterium tuberculosis infection by a subset of lung parenchyma-homing CD4 T cells. *The Journal of Immunology* 192: 2965–2969. [PubMed: 24591367]
55. Bull NC, Stylianou E, Kaveh DA, Pinpathomrat N, Pasricha J, Harrington-Kandt R, Garcia-Pelayo MC, Hogarth PJ, and McShane H. 2019. Enhanced protection conferred by mucosal BCG vaccination associates with presence of antigen-specific lung tissue-resident PD-1(+) KLRG1(–) CD4(+) T cells. *Mucosal Immunol* 12: 555–564. [PubMed: 30446726]
56. Gordon SN, Klatt NR, Bosinger SE, Brenchley JM, Milush JM, Engram JC, Dunham RM, Paiardini M, Klucking S, and Danesh A. 2007. Severe depletion of mucosal CD4+ T cells in AIDS-free simian immunodeficiency virus-infected sooty mangabeys. *The Journal of Immunology* 179: 3026–3034. [PubMed: 17709517]
57. Poles MA, Barsoum S, Yu W, Yu J, Sun P, Daly J, He T, Mehandru S, Talal A, Markowitz M, Hurley A, Ho D, and Zhang L. 2003. Human immunodeficiency virus type 1 induces persistent changes in mucosal and blood gammadelta T cells despite suppressive therapy. *J Virol* 77: 10456–10467. [PubMed: 12970431]
58. Li H, Peng H, Ma P, Ruan Y, Su B, Ding X, Xu C, Pauza CD, and Shao Y. 2008. Association between Vgamma2Vdelta2 T cells and disease progression after infection with closely related strains of HIV in China. *Clin Infect Dis* 46: 1466–1472. [PubMed: 18419457]
59. Chaudhry S, Cairo C, Venturi V, and Pauza CD. 2013. The  $\gamma\delta$  T-cell receptor repertoire is reconstituted in HIV patients after prolonged antiretroviral therapy. *Aids* 27: 1557–1562. [PubMed: 23525030]

**Key points:**

IV BCG induces a strong and sustained influx of mycobacteria-specific T cells, including polyfunctional CD4<sup>+</sup> and CD8 $\alpha\beta$ <sup>+</sup> T cells expressing cytokines and CD8 $\alpha\beta$ <sup>+</sup> and NK<sup>+</sup> cytotoxic effectors in the airways. IV BCG exhibited significantly higher numbers of tissue-resident memory T cells (TRM) in the lungs than ID BCG in SIV+MCM.

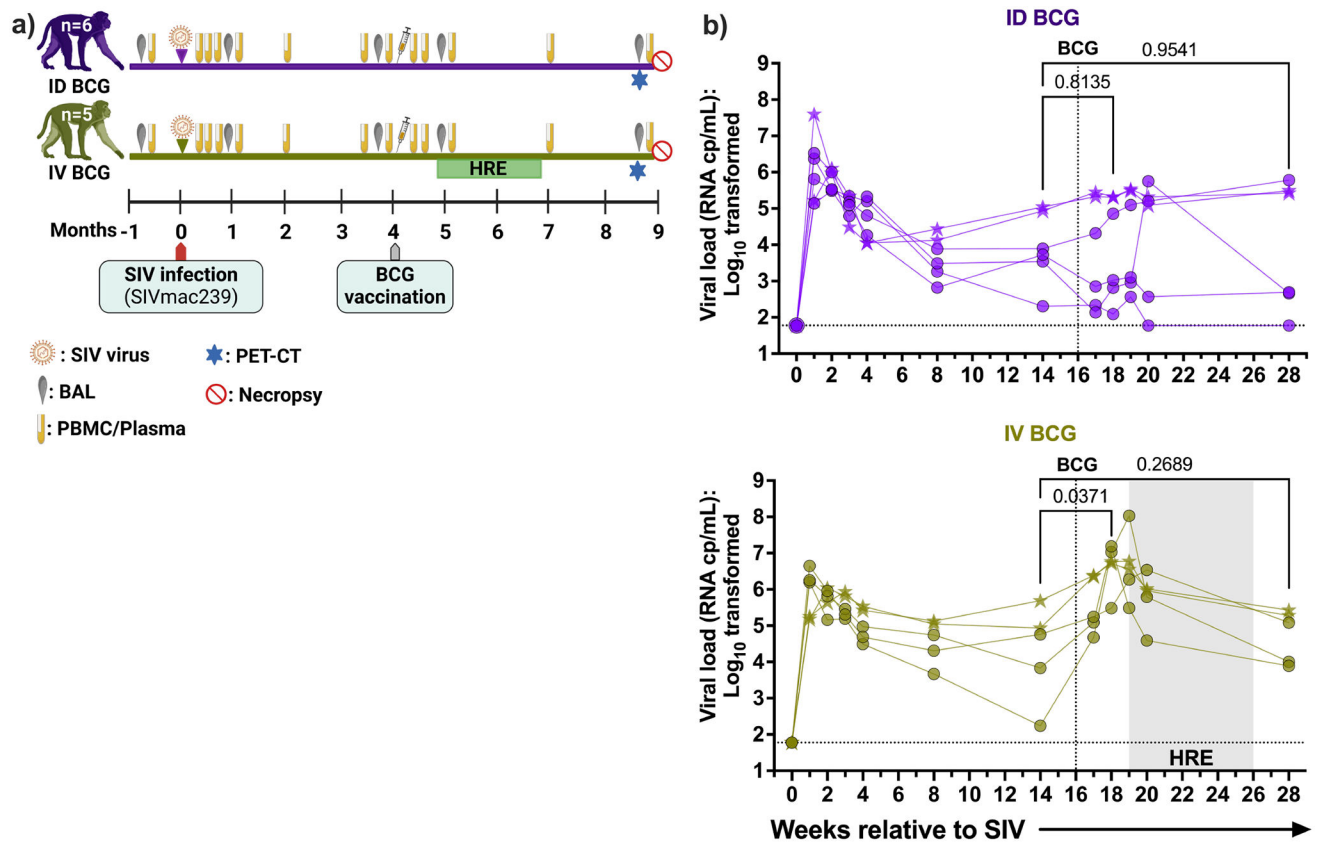


**Figure 1: Study design and SIV plasma viremia.**

**a)** Study design indicating SIV infection, BCG vaccination, HRE treatment, serial BAL and blood collection, and PET-CT time points. **b)** Quantification of plasma viral copy equivalents over time in MCM vaccinated with ID BCG (top panel, purple; n=6) or IV BCG (bottom panel, green; n=5). The horizontal dashed line represents the LOQ of ~62 copies/mL. Plasma viral load of each group was assessed by comparing two weeks before BCG vaccination to two- or 12-weeks after BCG vaccination using mixed-effects model with uncorrected Fisher's LSD p-values reported. Each symbol represents an individual animal. SIV controllers and non-controllers (baseline  $>10^5$  copies/mL) are indicated by circles and stars, respectively.

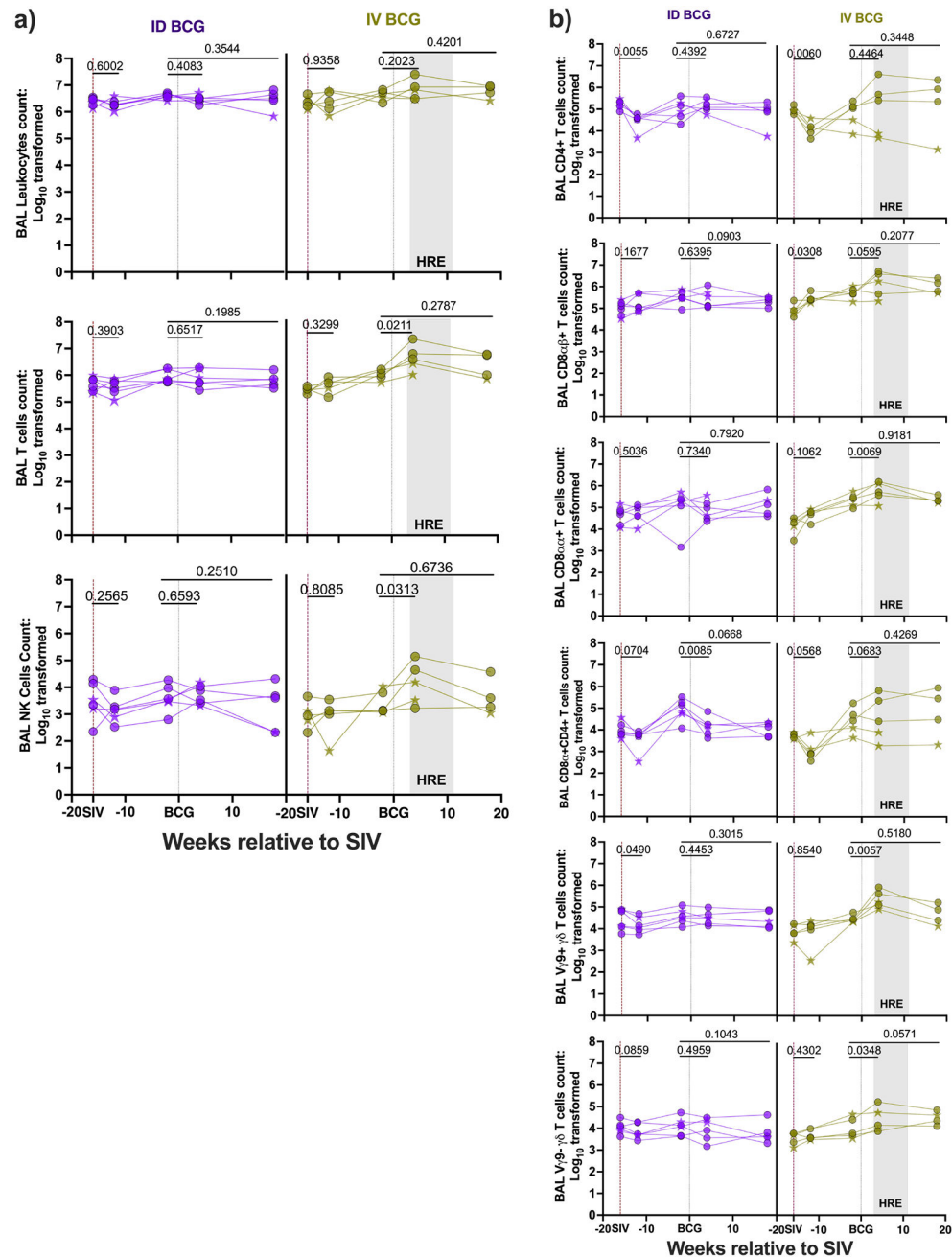


**Figure 2: Immune cell composition in airways during SIV infection and BCG vaccination.**  
**a)** Numbers of total leukocytes, T and NK cells in BAL. **b)** Numbers of T cell subsets in BAL. Each point represents an individual BAL with SIV non-controllers indicated by stars. Mixed-effects model with uncorrected Fisher's LSD p-values (Table 1) are shown.



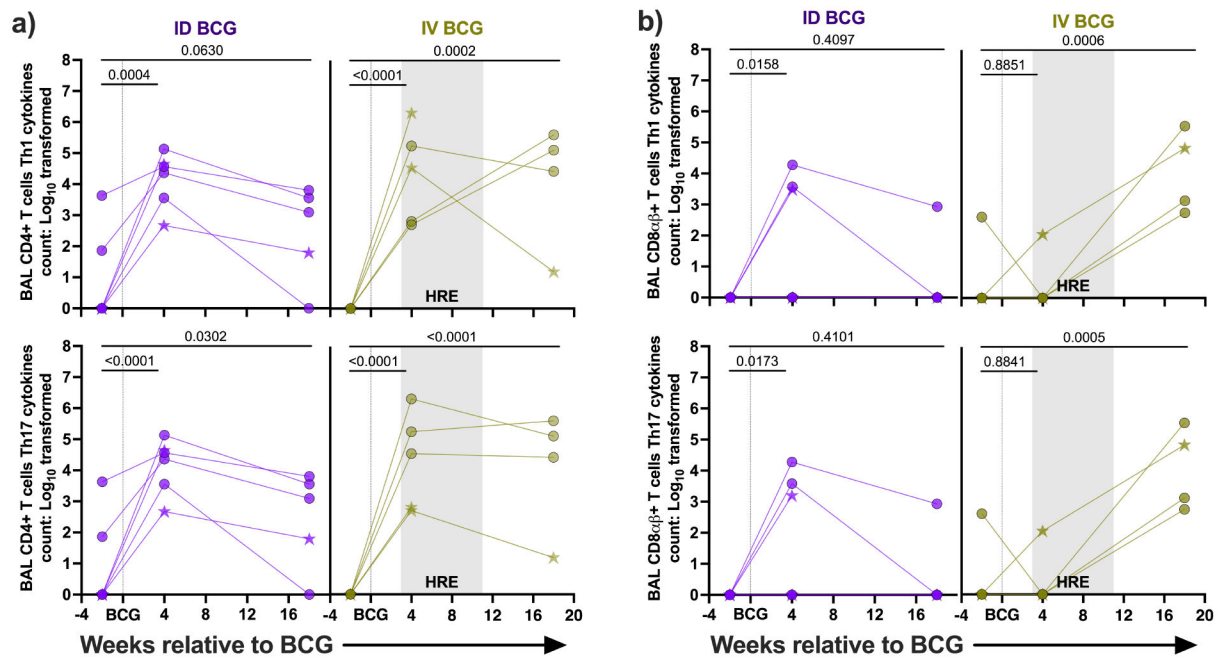


**Figure 3: T cell cytokines in airways following BCG vaccination.**

(a and b) Number of CD4+ (a) and CD8αβ+ (b) T cells making mycobacterial-specific Th1- and Th17-associated cytokines in airways.

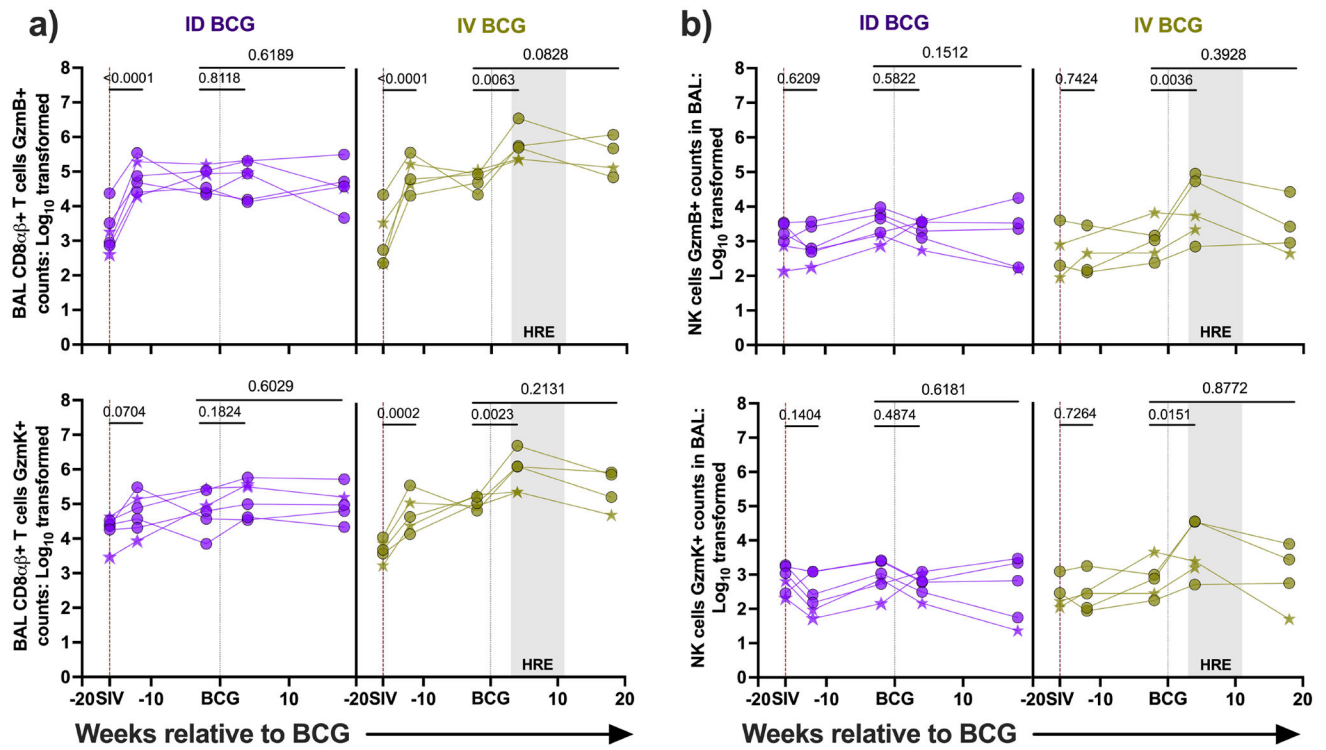


**Figure 4: CD8αβ+ T cells and NK cells cytotoxic effector in airways.**

(a and b) Number of CD8αβ+ T cells (a) and NK cells (b) producing GzmB and GzmK in airways.

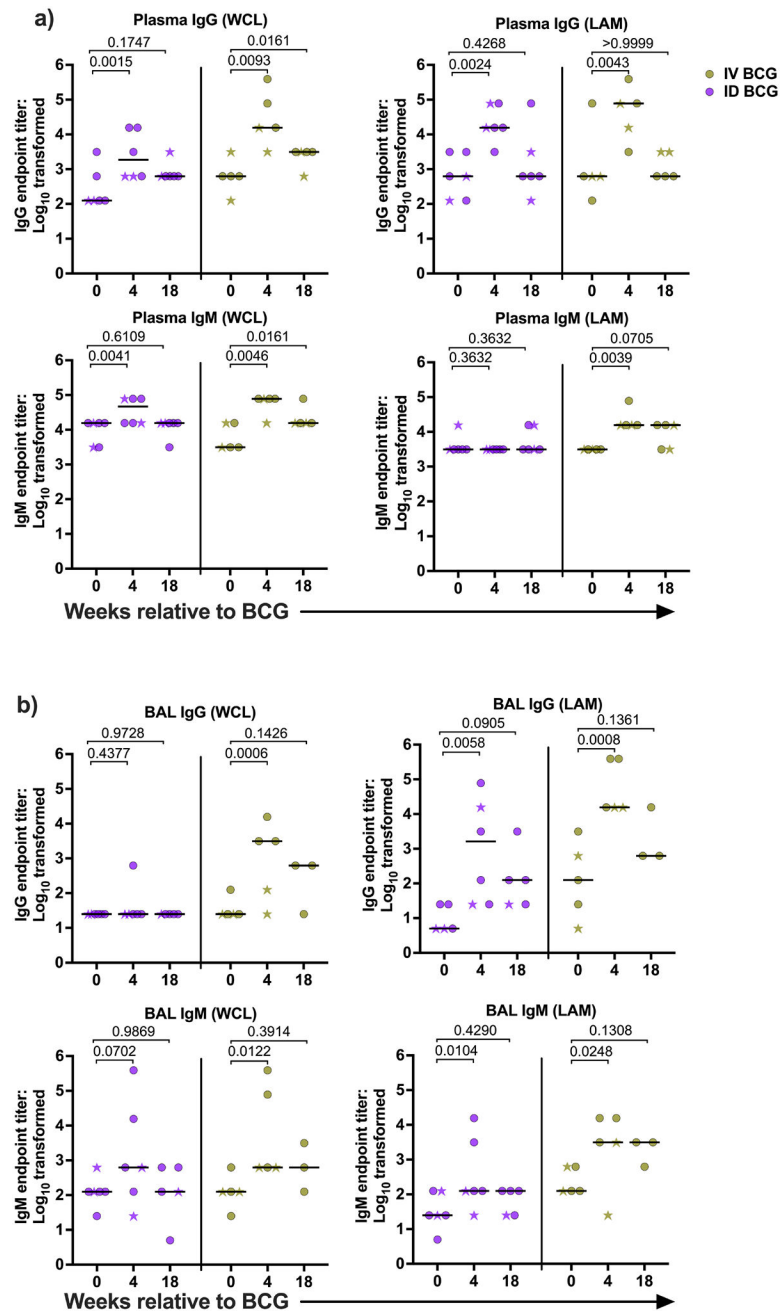


**Figure 5: Mycobacteria-specific antibodies in BAL and plasma following BCG vaccination.** IgG and IgM that bind WCL or LAM in plasma (a) and BALF (b). SIV non-controllers are indicated by stars. Mixed-effects model with uncorrected Fisher's LSD p-values in Table 2 represents group comparison.

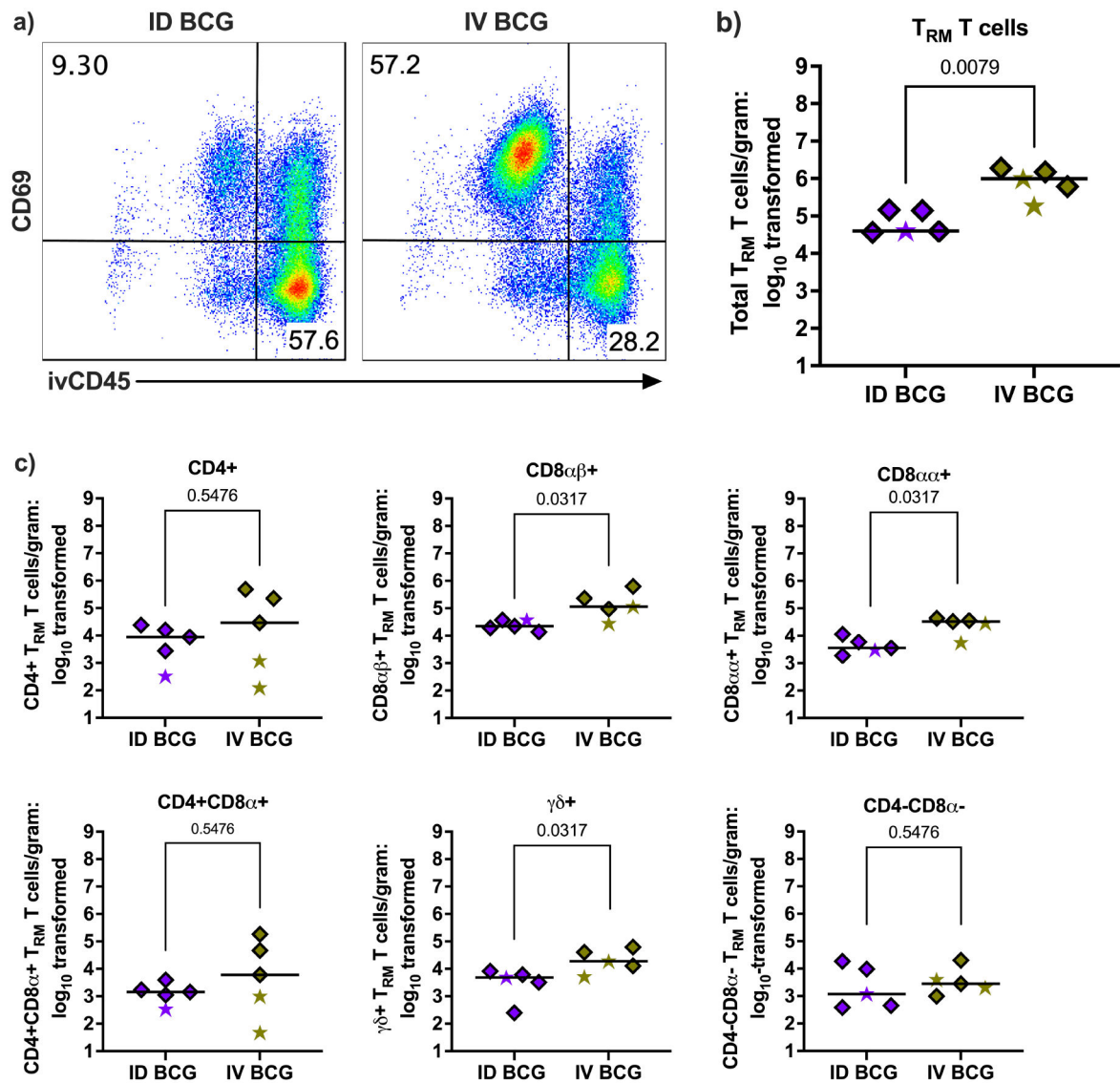


**Figure 6: T<sub>RM</sub> cell responses in lungs 20 weeks after BCG vaccination.**

Tissue-resident T cells (ivCD45-) are delineated from vascular-resident cells (ivCD45+).

**a)** T<sub>RM</sub> gating schematic, **b)** The number of T<sub>RM</sub> cells in lung tissue harvested 20 weeks after IV or ID BCG vaccination. **c)** The number of T<sub>RM</sub> cell subsets in lung tissue. SIV non-controllers are depicted by stars. Each symbol represents the mean value from 3 lung lobes per animal. Mann-Whitney p-values are reported.

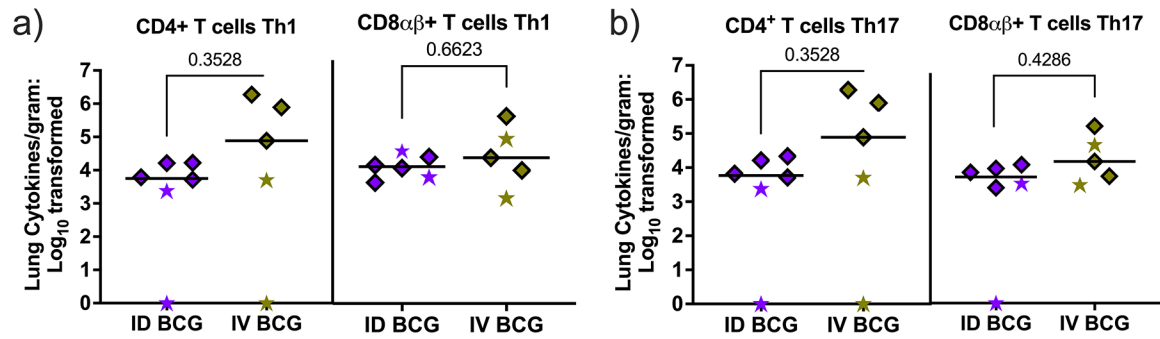


**Figure 7: Cytokines responses in lungs 20 weeks after BCG vaccination.**

The number of CD4+ and CD8αβ+ T cells in the lung that make any **a)** Th1- and Th1-(IFN $\gamma$ , IL-2, TNF), and, **b)** Th17- and Th17- (IFN $\gamma$ , IL-2, IL-17, TNF) associated cytokines. SIV non-controllers are depicted by stars. Each symbol represents the mean value from 3 lung lobes per animal. Mann-Whitney p-values are reported.

**Table 1:**

Mixed model analysis comparing cellular immune response elicited by ID BCG versus IV BCG vaccination routes at different time points.

Cells	ID BCG vs. IV BCG	P-value	Mean Difference: ID BCG - IV BCG (95% CI)
T cells subsets	PreBCG	0.6362 ns	
	CD4+ 4 week post BCG	0.9049 ns	
	18 Weeks post BCG	0.5927 ns	
	PreBCG	0.2352 ns	
	CD8αβ+ 4 week post BCG	0.0623 #	−0.6931 (−1.433 to 0.04675)
	18 Weeks post BCG	0.0147 *	−0.694 (−1.180 to −0.2082)
	PreBCG	0.4007 ns	
	CD8αα+ 4 week post BCG	0.0113 *	−0.8719 (−1.491 to −0.2524)
	18 Weeks post BCG	0.3385 ns	
	PreBCG	0.1738 ns	
	CD8α+CD4+ 4 week post BCG	0.441 ns	
	18 Weeks post BCG	0.2789 ns	
	PreBCG	0.5546 ns	
	Vg9+γδ 4 week post BCG	0.0053 **	−0.8599 (−1.374 to −0.3453)
	18 Weeks post BCG	0.4764 ns	
Th1 associated cytokines	PreBCG	0.8549 ns	
	Vg9-γδ 4 week post BCG	0.2264 ns	
	18 Weeks post BCG	0.0359 *	−0.7162 (−1.370 to −0.0629)
	PreBCG	0.2809 ns	
	CD4+ 4 weeks post BCG	0.8427 ns	
	18 weeks post BCG	0.0728 #	−1.716 (−3.602 to 0.1708)
Th17 associated cytokines	PreBCG	0.5155 ns	
	CD8αβ+ 4 weeks post BCG	0.0737 #	1.478 (−0.1528 to 3.109)
	18 weeks post BCG	0.0006 ***	−3.413 (−5.214 to −1.612)
	PreBCG	0.2779 ns	
	CD4+ 4 weeks post BCG	0.8405 ns	
	18 weeks post BCG	0.0962 #	−1.543 (−3.381 to 0.2954)
CD8αβ+ T cells cytotoxic molecules	PreBCG	0.5117 ns	
	CD8αβ+ 4 weeks post BCG	0.0799 #	1.433 (−0.1835 to 3.049)
	18 weeks post BCG	0.0006 ***	−3.414 (−5.199 to −1.630)
	PreBCG	0.8686 ns	
	GzmB 4 weeks post BCG	0.0074 **	−0.9387 (−1.612 to −0.2649)
	18 weeks post BCG	0.0279 *	−0.8393 (−1.583 to −0.0958)
NK cells cytotoxic molecules	PreBCG	0.3898 ns	
	GzmK 4 weeks post BCG	0.0109 *	−0.804 (−1.413 to −0.1947)
	18 weeks post BCG	0.1463 ns	



Cells	ID BCG vs. IV BCG	P-value	Mean Difference: ID BCG - IV BCG (95% CI)
	4 weeks post BCG	0.1133	ns
	18 weeks post BCG	0.5675	ns
	PreBCG	0.7972	ns
	GzmK 4 weeks post BCG	0.0173	* -0.9372 (-1.700 to -0.1746)
	18 weeks post BCG	0.3412	ns

ID and IV BCG were compared at each time point for each cell type. Fisher's LSD test p-values reported. For p-values < 0.10, the mean difference of ID BCG - IV BCG is shown with 95% confidence interval. The summary of p-value is presented; ns: not significant,

#. 0.05 < p < 0.10,

\*. p < 0.05,

\*\*. p < 0.01 and

\*\*\*. p < 0.001.

GzmB: Granzyme B and GzmK: Granzyme K

**Table 2:**

Mixed model analysis comparing the humoral immune response elicited in the plasma and airways by ID BCG versus IV BCG at different time points.

Niche	Immunoglobulin	ID BCG vs. IV BCG	P-value	Mean Difference: ID BCG - IV BCG (95% CI)
Plasma	IgG WCL	PreBCG	0.3107	ns
		4 weeks post BCG	0.0421	*
		18 weeks post BCG	0.04	*
	IgM WCL	PreBCG	0.432	ns
		4 weeks post BCG	0.3434	ns
		18 weeks post BCG	0.1954	ns
	IgG LAM	PreBCG	0.5487	ns
		4 weeks post BCG	0.5161	ns
		18 weeks post BCG	0.8804	ns
	IgM LAM	PreBCG	0.3632	ns
		4 weeks post BCG	0.0039	**
		18 weeks post BCG	0.432	ns
BAL (airway)	IgG WCL	PreBCG	0.7060	ns
		4 weeks post BCG	0.0016	**
		18 weeks post BCG	0.1002	ns
	IgM WCL	PreBCG	>0.9999	ns
		4 weeks post BCG	0.3160	ns
		18 weeks post BCG	0.4222	ns
	IgG LAM	PreBCG	0.0878	#
		4 weeks post BCG	0.006	**
		18 weeks post BCG	0.0222	*
	IgM LAM	PreBCG	0.0727	#
		4 weeks post BCG	0.0975	#
		18 weeks post BCG	0.0240	*

ID and IV BCG were compared at each time point for each cell type. Fisher's LSD test p-values reported. For p-values < 0.10, the mean difference of ID BCG - IV BCG is shown with 95% confidence interval. The summary of p-value is presented;

#. 0.05 < p < 0.10,

\*. p < 0.05,

\*\*. p < 0.01 and

\*\*\*. p < 0.001.

WCL: H37Rv whole cell lysate, LAM: Lipoarabinomannan.